EUROPEAN ORGANIZATION FOR NUCLEAR RESEARCH

CERN-PPE/94-208
December 12, 1994

Study of the Subjet Structure of Quark and Gluon Jets

The ALEPH Collaboration

Abstract

Measurements of the subjet structure of quark and gluon jets in hadronic Z decays are presented. The analysis is based on one million hadronic events recorded by the ALEPH detector. Roughly symmetric three-jet events are selected with a coarse jet-resolution cut-off, y_1. Gluon jets are identified with a purity of 94.6% in those events where evidence of long-lived heavy-flavour hadrons in the other two jets is found. The jets are then analyzed using a smaller cut-off y_0 ($< y_1$) so that subjets are resolved. The properties of the jets (subjet multiplicities $\langle N_q \rangle$, $\langle N_g \rangle$ and rates $R_n^{g(q)}$ for $n = 1, 2, 3, 4$) are determined and are found to be in good agreement with the expectations of perturbative QCD as long as the subjet resolution parameter y_0 is sufficiently large to keep non-perturbative effects small. In particular, the ratio $\langle N_g - 1 \rangle / \langle N_q - 1 \rangle$, which to leading order in QCD is given by the ratio of colour factors $C_A/C_F = 9/4$, is measured to be 1.96 ± 0.15 for $y_0 = 2 \cdot 10^{-3}$, but falls to 1.29 ± 0.03 for $y_0 = 1.6 \cdot 10^{-5}$.

Submitted to Physics Letters B

The ALEPH Collaboration

D. Buskulic, D. Casper, I. De Bonis, D. Decamp, P. Ghez, C. Goy, J.-P. Lees, M.-N. Minard, P. Odier, B. Pietrzyk

Laboratoire de Physique des Particules (LAPP), IN^{2}P^3-CNRS, 74019 Annecy-le-Vieux Cedex, France

F. Ariztizabal, M. Chmeissani, J.M. Crespo, I. Efthymiopoulos, E. Fernandez, M. Fernandez-Bosman, V. Gaitan, Ll. Garrido,[15] M. Martinez, S. Orteu, A. Pacheco, C. Padilla, F. Palla, A. Pascual, J.A. Perlas, F. Sanchez, F. Teubert

Institut de Fisica d'Altes Energies, Universitat Autonoma de Barcelona, 08193 Bellaterra (Barcelona), Spain[7]

D. Creanza, M. de Palma, A. Farilla, G. Iaselli, G. Maggi,[3] N. Marinelli, S. Natali, S. Nuzzo, A. Ranieri, G. Raso, F. Romano, F. Ruggieri, G. Selvaggi, L. Silvestris, P. Tempesta, G. Zito

Dipartimento di Fisica, INFN Sezione di Bari, 70126 Bari, Italy

X. Huang, J. Lin, Q. Ouyang, T. Wang, Y. Xie, R. Xu, S. Xue, J. Zhang, L. Zhang, W. Zhao

Institute of High-Energy Physics, Academia Sinica, Beijing, The People's Republic of China[8]

G. Bonvicini, M. Cattaneo, P. Comas, P. Coyle, H. Drevermann, A. Engelhardt, R.W. Forty, M. Frank, G. Ganis, M. Girone, R. Hagelberg, J. Harvey, R. Jacobsen,[24] B. Jost, J. Knobloch, I. Lehraus, M. Maggi, C. Markou,[27] E.B. Martin, P. Mato, H. Meinhard, A. Minten, R. Miquel, P. Palazzi, J.R. Pater, P. Perrodo, J.-F. Pusztaszeri, F. Ranjard, L. Rolandi, D. Schlatter, M. Schmelling, W. Tejessy, I.R. Tomalin, R. Veenhof, A. Venturi, H. Wachsmuth, W. Wiedenmann, T. Wildish, W. Witzeling, J. Wotschack

European Laboratory for Particle Physics (CERN), 1211 Geneva 23, Switzerland

Z. Ajaltouni, M. Bardadin-Otwinowska,[2] A. Barres, C. Boyer, A. Falvard, P. Gay, C. Guicheney, P. Henrard, J. Jousset, B. Michel, S. Monteil, J-C. Montret, D. Pallin, P. Perret, F. Podlyski, J. Proriol, J.-M. Rossignol, F. Saadi

Laboratoire de Physique Corpusculaire, Université Blaise Pascal, IN^{2}P^3-CNRS, Clermont-Ferrand, 63177 Aubière, France

T. Fearnley, J.B. Hansen, J.D. Hansen, J.R. Hansen, P.H. Hansen, S.D. Johnson, B.S. Nilsson

Niels Bohr Institute, 2100 Copenhagen, Denmark[9]

A. Kyriakis, E. Simopoulou, I. Siotis, A. Vayaki, K. Zachariadou

Nuclear Research Center Demokritos (NRCD), Athens, Greece

A. Blondel, G. Bonneaud, J.C. Brient, P. Bourdon, L. Passalacqua, A. Rougé, M. Rumpf, R. Tanaka, A. Valassi, M. Verderi, H. Videau

Laboratoire de Physique Nucléaire et des Hautes Energies, Ecole Polytechnique, IN^{2}P^3-CNRS, 91128 Palaiseau Cedex, France

D.J. Candlin, M.I. Parsons, E. Veitch

Department of Physics, University of Edinburgh, Edinburgh EH9 3JZ, United Kingdom[10]

E. Focardi, G. Parrini

Dipartimento di Fisica, Università di Firenze, INFN Sezione di Firenze, 50125 Firenze, Italy

M. Corden, M. Delfino,[12] C. Georgiopoulos, D.E. Jaffe

Supercomputer Computations Research Institute, Florida State University, Tallahassee, FL 32306-4052, USA [13,14]

A. Antonelli, G. Bencivenni, G. Bologna,[4] F. Bossi, P. Campana, G. Capon, F. Cerutti, V. Chiarella, G. Felici, P. Laurelli, G. Mannocchi,[5] F. Murtas, G.P. Murtas, M. Pepe-Altarelli, S. Salomone

Laboratori Nazionali dell'INFN (LNF-INFN), 00044 Frascati, Italy

P. Colrain, I. ten Have,[6] I.G. Knowles, J.G. Lynch, W. Maitland, W.T. Morton, C. Raine, P. Reeves, J.M. Scarr, K. Smith, M.G. Smith, A.S. Thompson, S. Thorn, R.M. Turnbull

Department of Physics and Astronomy, University of Glasgow, Glasgow G12 8QQ,United Kingdom[10]

U. Becker, O. Braun, C. Geweniger, G. Graefe, P. Hanke, V. Hepp, E.E. Kluge, A. Putzer, B. Rensch, M. Schmidt, J. Sommer, H. Stenzel, K. Tittel, M. Wunsch

Institut für Hochenergiephysik, Universität Heidelberg, 69120 Heidelberg, Fed. Rep. of Germany[16]

R. Beuselinck, D.M. Binnie, W. Cameron, D.J. Colling, P.J. Dornan, N. Konstantinidis, L. Moneta, A. Moutoussi, J. Nash, G. San Martin, J.K. Sedgbeer, A.M. Stacey

Department of Physics, Imperial College, London SW7 2BZ, United Kingdom[10]

G. Dissertori, P. Girtler, E. Kneringer, D. Kuhn, G. Rudolph

Institut für Experimentalphysik, Universität Innsbruck, 6020 Innsbruck, Austria[18]

C.K. Bowdery, T.J. Brodbeck, A.J. Finch, F. Foster, G. Hughes, D. Jackson, N.R. Keemer, M. Nuttall, A. Patel, T. Sloan, S.W. Snow, E.P. Whelan

Department of Physics, University of Lancaster, Lancaster LA1 4YB, United Kingdom[10]

A. Galla, A.M. Greene, K. Kleinknecht, J. Raab, B. Renk, H.-G. Sander, H. Schmidt, S.M. Walther, R. Wanke, B. Wolf

Institut für Physik, Universität Mainz, 55099 Mainz, Fed. Rep. of Germany[16]

J.J. Aubert, A.M. Bencheikh, C. Benchouk, A. Bonissent, G. Bujosa, D. Calvet, J. Carr, C. Diaconu, F. Etienne, M. Thulasidas, D. Nicod, P. Payre, D. Rousseau, M. Talby

Centre de Physique des Particules, Faculté des Sciences de Luminy, IN^{2}P^3-CNRS, 13288 Marseille, France

I. Abt, R. Assmann, C. Bauer, W. Blum, D. Brown,[24] H. Dietl, F. Dydak,[21] C. Gotzhein, A.W. Halley, K. Jakobs, H. Kroha, G. Lütjens, G. Lutz, W. Männer, H.-G. Moser, R. Richter, A. Rosado-Schlosser, A.S. Schwarz,[23] R. Settles, H. Seywerd, U. Stierlin,[2] R. St. Denis, G. Wolf

Max-Planck-Institut für Physik, Werner-Heisenberg-Institut, 80805 München, Fed. Rep. of Germany[16]

R. Alemany, J. Boucrot, O. Callot, A. Cordier, F. Courault, M. Davier, L. Duflot, J.-F. Grivaz, Ph. Heusse, M. Jacquet, P. Janot, D.W. Kim,[19] F. Le Diberder, J. Lefrançois, A.-M. Lutz, G. Musolino, I. Nikolic, H.J. Park, I.C. Park, M.-H. Schune, S. Simion, J.-J. Veillet, I. Videau

Laboratoire de l'Accélérateur Linéaire, Université de Paris-Sud, IN^{2}P^3-CNRS, 91405 Orsay Cedex, France

D. Abbaneo, G. Bagliesi, G. Batignani, S. Bettarini, U. Bottigli, C. Bozzi, G. Calderini, M. Carpinelli, M.A. Ciocci, V. Ciulli, R. Dell'Orso, I. Ferrante, F. Fidecaro, L. Foà,[1] F. Forti, A. Giassi, M.A. Giorgi, A. Gregorio, F. Ligabue, A. Lusiani, P.S. Marrocchesi, A. Messineo, G. Rizzo, G. Sanguinetti, A. Sciabà, P. Spagnolo, J. Steinberger, R. Tenchini, G. Tonelli,[26] G. Triggiani, C. Vannini, P.G. Verdini, J. Walsh

Dipartimento di Fisica dell'Università, INFN Sezione di Pisa, e Scuola Normale Superiore, 56010 Pisa, Italy

A.P. Betteridge, G.A. Blair, L.M. Bryant, Y. Gao, M.G. Green, D.L. Johnson, T. Medcalf, Ll.M. Mir, J.A. Strong

Department of Physics, Royal Holloway & Bedford New College, University of London, Surrey TW20 OEX, United Kingdom[10]

V. Bertin, D.R. Botterill, R.W. Clifft, T.R. Edgecock, S. Haywood, M. Edwards, P. Maley, P.R. Norton, J.C. Thompson

Particle Physics Dept., Rutherford Appleton Laboratory, Chilton, Didcot, Oxon OX11 OQX, United Kingdom[10]

B. Bloch-Devaux, P. Colas, H. Duarte, S. Emery, W. Kozanecki, E. Lançon, M.C. Lemaire, E. Locci, B. Marx, P. Perez, J. Rander, J.-F. Renardy, A. Rosowsky, A. Roussarie, J.-P. Schuller, J. Schwindling, D. Si Mohand, A. Trabelsi, B. Vallage

CEA, DAPNIA/Service de Physique des Particules, CE-Saclay, 91191 Gif-sur-Yvette Cedex, France[17]

R.P. Johnson, A.M. Litke, G. Taylor, J. Wear

Institute for Particle Physics, University of California at Santa Cruz, Santa Cruz, CA 95064, USA[22]

A. Beddall, C.N. Booth, R. Boswell, S. Cartwright, F. Combley, I. Dawson, A. Koksal, M. Letho, W.M. Newton, C. Rankin, L.F. Thompson

Department of Physics, University of Sheffield, Sheffield S3 7RH, United Kingdom[10]

A. Böhrer, S. Brandt, G. Cowan, E. Feigl, C. Grupen, G. Lutters, J. Minguet-Rodriguez, F. Rivera,[25] P. Saraiva, U. Schäfer, L. Smolik

Fachbereich Physik, Universität Siegen, 57068 Siegen, Fed. Rep. of Germany[16]

L. Bosisio, R. Della Marina, G. Giannini, B. Gobbo, L. Pitis, F. Ragusa[20]

Dipartimento di Fisica, Università di Trieste e INFN Sezione di Trieste, 34127 Trieste, Italy

H. Kim, J. Rothberg, S. Wasserbaech

Experimental Elementary Particle Physics, University of Washington, WA 98195 Seattle, U.S.A.

S.R. Armstrong, L. Bellantoni, P. Elmer, Z. Feng, D.P.S. Ferguson, Y.S. Gao, S. González, J. Grahl, J.L. Harton, O.J. Hayes, H. Hu, P.A. McNamara III, J.M. Nachtman, W. Orejudos, Y.B. Pan, Y. Saadi, M. Schmitt, I.J. Scott, V. Sharma, J.D. Turk, A.M. Walsh, F.V. Weber,[1] Sau Lan Wu, X. Wu, J.M. Yamartino, M. Zheng, G. Zobernig

Department of Physics, University of Wisconsin, Madison, WI 53706, USA[11]

[1] Now at CERN, 1211 Geneva 23, Switzerland.
[2] Deceased.
[3] Now at Dipartimento di Fisica, Università di Lecce, 73100 Lecce, Italy.
[4] Also Istituto di Fisica Generale, Università di Torino, Torino, Italy.
[5] Also Istituto di Cosmo-Geofisica del C.N.R., Torino, Italy.
[6] Now at TSM Business School, Enschede, The Netherlands.
[7] Supported by CICYT, Spain.
[8] Supported by the National Science Foundation of China.
[9] Supported by the Danish Natural Science Research Council.
[10] Supported by the UK Science and Engineering Research Council.
[11] Supported by the US Department of Energy, contract DE-AC02-76ER00881.
[12] On leave from Universitat Autonoma de Barcelona, Barcelona, Spain.
[13] Supported by the US Department of Energy, contract DE-FG05-92ER40742.
[14] Supported by the US Department of Energy, contract DE-FC05-85ER250000.
[15] Permanent address: Universitat de Barcelona, 08208 Barcelona, Spain.
[16] Supported by the Bundesministerium für Forschung und Technologie, Fed. Rep. of Germany.
[17] Supported by the Direction des Sciences de la Matière, C.E.A.
[18] Supported by Fonds zur Förderung der wissenschaftlichen Forschung, Austria.
[19] Permanent address: Kangnung National University, Kangnung, Korea.
[20] Now at Dipartimento di Fisica, Università di Milano, Milano, Italy.
[21] Also at CERN, 1211 Geneva 23, Switzerland.
[22] Supported by the US Department of Energy, grant DE-FG03-92ER40689.
[23] Now at DESY, Hamburg, Germany.
[24] Now at Lawrence Berkeley Laboratory, Berkeley, CA 94720, USA.
[25] Partially supported by Colciencias, Colombia.
[26] Also at Istituto di Matematica e Fisica, Università di Sassari, Sassari, Italy.
[27] Now at University of Athens, 157-71 Athens, Greece.

1. Introduction

The large number of events of the type $e^+e^- \to hadrons$ available from the ALEPH experiment at LEP provides an opportunity to investigate the detailed structure of hadronic final states. In this letter, measurements are presented of subjet rates and multiplicities in identified quark and gluon jets from three-jet events. Comparisons with theoretical predictions indicate that these quantities are sensitive to the colour structure of the underlying quark and gluon interactions.

Jets in an event are defined with an iterative clustering procedure (the "Durham" algorithm [1]). For each pair of particles i and j in the event, one defines the quantity y_{ij}

$$y_{ij} = \frac{2\,min(E_i^2, E_j^2)(1 - cos\theta_{ij})}{E_{vis}^2} \ , \tag{1}$$

where E_i and E_j are the particles' energies, θ_{ij} is the opening angle of the pair, and E_{vis} is the total visible energy in the event. The pair with the smallest value of y_{ij} is replaced by a pseudoparticle (cluster). The four-momentum of the cluster is taken to be the sum of the four momenta of particles i and j (the "E" recombination scheme). The procedure is repeated until all of the y_{ij} are greater than a given threshold, y_{cut} (the jet resolution parameter). The number of jets is defined to be the number of remaining clusters.

First, three-jet events are selected using an initial value of the resolution parameter, $y_1 = 0.1$. This leads to three well separated jets of approximately equal energy. Such an event configuration arises predominantly from the radiation of a single hard gluon from the original quark antiquark pair. Perturbative QCD predicts that the probability for an additional gluon to be radiated from the quark is proportional to the colour factor $C_F = 4/3$, whereas gluon radiation from a gluon is proportional to the factor $C_A = 3$ (see e.g. reference [2]). This results in distinct predictions for the internal structure of quark and gluon jets.

In order to investigate this internal structure, the particles of the individual jets are clustered using a smaller value of the resolution parameter y_0 ($< y_1$) so that subjets are resolved. Several properties of quark and gluon jets are measured as a function of y_0, including the mean subjet multiplicity, $\langle N_{g(q)}(y_0)\rangle$ and n-subjet rates $R_n^{g(q)}(y_0)$ for $n = 1, 2, 3, 4$. This technique for forming subjets was first investigated theoretically [3] and experimentally [4, 5, 6] in studies without identification of the quark and gluon jets.

2. Event and Jet Selection

The data used were recorded by the ALEPH detector in 1992 and 1993 at a centre-of-mass energy of $E_{cm} = 91.2$ GeV. A detailed description of the ALEPH detector is given in reference [7]. The measurements presented here are based on both charged particle measurements from the time projection chamber, inner tracking chamber, and vertex detector, as well as information on charged and neutral particles from the electromagnetic and hadronic calorimeters. An energy-flow reconstruction algorithm is applied, which takes advantage of the redundancy of energy and momentum measurements and exploits photon, electron and muon identification [8]. The output of this algorithm is a list of "energy flow objects", with measured momentum vectors, which are used as input to the jet clustering algorithm.

A preselection of events is made by requiring at least 5 charged tracks and 20 GeV of visible energy in the detector. This procedure results in a sample of 988461 candidate hadronic events. From these, three-jet events are selected according to the Durham algorithm with a value of the jet resolution parameter $y_1 = 0.1$. In order that most of the particles of a jet pass through the vertex detector, it is required that each jet has an angle of at least 35° with respect to the beam axis. To reject events of the type $q\overline{q}\gamma$, an event is not accepted if more than 85% of the energy of a jet is carried by a single photon. This results in a sample of 28350 three-jet events, with no

significant background from other event types such as $\tau^+\tau^-$ final states or two-photon collisions. Because of the high value of y_1, the jets are well separated and of approximately equal energy. The distribution of the smallest separation angle between jets for the selected three-jet events is shown in figure 1(a).

From the selected events, the observables being studied are measured using two sets of jets. In the following the variable X will be used to represent one of the possible observables, i.e. mean subjet multiplicities or n-subjet rates. The first set simply consists of all the jets in the three-jet sample, which is a mixture of 2/3 quark and 1/3 gluon jets. In the following a measured quantity from this sample will be referred to with the subscript *mix*. The second set of jets is obtained by requiring evidence of long-lived hadrons in two of the jets (indicating b or c-quark jets) based on precision tracking information from the silicon vertex detector. These two jets are rejected and the third is taken as a candidate gluon jet. Quantities based on this set of jets will be referred to with the subscript *tag*. The distributions of jet energies for the tagged and mixed jet samples are shown in figure 1(b).

The general technique for the tagging of heavy-quark jets is based on a three-dimensional impact parameter measured for each charged-particle track. This is described in detail in reference [9], where it is shown that the systematic uncertainty in the purity of a tagged heavy-quark jet sample is at the level of $1-2\%$. Based on the measured impact parameter and estimated resolution a quantity P_{jet} is constructed for each jet so as to be uniformly distributed between zero and one if all of the charged particles in the jet originate from the primary vertex. This distribution is sharply peaked near zero if the jet contains particles which do not, such as decay products of long lived hadrons containing b or c quarks. It is required that two of the three jets have a value of P_{jet} less than 0.01, and that the third jet has a probability greater than 0.01. According to Monte Carlo studies based on the JETSET model version 7.3 [10] plus detector simulation, only 2% of the gluon jets have $P_{jet} < 0.01$, which arises in part from production of a secondary $b\overline{b}$ pair in the gluon jet. The bias introduced in the gluon jet sample by requiring $P_{jet} > 0.01$ is therefore small. These selection criteria result in a sample of 1750 tagged gluon-jet candidates.

The purity of the tagged gluon-jet sample is determined by the following procedure. The program JETSET is used to generate a system of partons (quarks and gluons) according to the parton-shower picture of QCD, which is then converted into a system of hadrons by means of a string model. The hadrons are processed by the detector-simulation program and then by the same reconstruction algorithms as used for the real data. The jet clustering algorithm is first applied to the parton-level information provided by the Monte Carlo generator, in such a way that three clusters are always formed for each event. The quark and antiquark jets are identified as those containing the original quark and antiquark from the Z decay, and the remaining jet is then the gluon jet. The jet analysis is then applied to the Monte Carlo data after detector simulation yielding a set of tagged gluon jet candidates. The parton-level jets are matched to the jets of detected hadrons by successively associating hadron-parton jet pairs with the smallest angular separation. For the standard cut used in this analysis ($P_{jet}^{cut} = 0.01$) the selection efficiency is 6.1% (i.e. fraction of three-jet events that yield a tagged gluon jet) and the gluon-jet purity is 94.6%.

Since a high value of y_1 was used, the three jets are well separated and the matching procedure results in angles between associated parton and hadron level jets that are small compared to the angular separation between different jets. In a negligibly small fraction of events (0.5%) the primary quark and antiquark are clustered into the same jet, resulting in an ambiguous event.

3. Corrections to the Data

Before determining the subjet multiplicities and rates for pure samples of quark and gluon jets, the measurements for the tagged and mixed jet samples are corrected for effects of geometrical acceptance, detector efficiency and resolution, decays, secondary interactions and initial state photon radiation. A first set of hadronic events was produced with the JETSET program followed by detector simulation (the same data set as for determination of the gluon-jet purity above). From these data (i.e. simulated energy-flow objects) the various observables (multiplicities, etc.) were computed, yielding X_{tag}^{MC+det} for the case of gluon-jet tagging and X_{mix}^{MC+det} for quantities computed from all jets in the selected three-jet events.

A second set of Monte Carlo data without detector simulation was generated, in which all particles with mean lifetimes less than 1 ns were required to decay, the others were treated as stable, and initial state radiation was turned off. The jet clustering algorithm was applied to all final state particles (including neutrinos) and three-jet events were selected with the resolution parameter $y_1 = 0.1$. In order to insure that these events originated from $q\overline{q}g$ and not $q\overline{q}\gamma$ configurations, events were rejected if more than 85% of the energy of a jet was carried by a single photon. From these events, quark and gluon jets were defined using the same procedure as that described in section 2; i.e. parton and hadron level jets (in the present case without detector simulation) were matched according to minimum separation angles. The observable quantities from the resulting quark and gluon jets were computed, and are referred to here as X_q^{gen} and X_g^{gen}.

The two Monte Carlo data sets, "generator only" and "full simulation and tagging procedure", were used to derive multiplicative correction factors for the observables, with separate corrections for both the mixed and tagged jet samples. The factors are computed as a function of the subjet resolution parameter y_0. The corrected quantities are given by

$$X_{j\ corrected} = X_{j\ measured} \cdot C_j \ , \tag{2}$$

where

$$C_j = \frac{p_j\, X_g^{gen} + (1-p_j)\, X_q^{gen}}{X_j^{MC+det}} \ , \tag{3}$$

and where the index j refers to the jet sample, mixed or tagged. For the mixed sample, the numerator of the correction factor corresponds to simply using all of the jets. This procedure corrects the measurements to a fixed centre-of-mass energy (free of initial state radiation) and a well defined final state particle composition for a fraction of p gluon jets and $1-p$ quark jets, for the two cases $p = p_{tag} = 0.946$ and $p = p_{mix} = 1/3$. The corrections remove small biases introduced by the tagging procedure, resulting for example from the fact that the quark jets in the tagged jet sample (i.e. the 5.4% that are misidentified as gluon jets) have a different flavour composition than the quark jets obtained by using all jets. The factors for the mean subjet multiplicities minus one $\langle N_g - 1\rangle$, $\langle N_q - 1\rangle$ and for the subjet rates are typically in the range $0.9 \leq C \leq 1.1$. The corrections for the two samples are very similar, differing only by a few percent.

From the tagged and mixed observables after application of the detector-correction factors, the corresponding quantities for pure quark and gluon jets, X_q and X_g, can be extracted by solving the following set of equations:

$$\begin{aligned} X_{tag} &= p_{tag}X_g + (1-p_{tag})X_q \\ X_{mix} &= p_{mix}X_g + (1-p_{mix})X_q \ . \end{aligned} \tag{4}$$

It was checked that the corrected jet multiplicities and rates are not sensitive to the selection criteria. The largest sensitivity was found to come from the cut on P_{jet}. Systematic errors have been estimated by repeating the analysis with this cut equal to half and twice the standard value of 0.01. A cut value of 0.005 gives a gluon purity $p_{tag} = 0.968$ and 0.02 gives $p_{tag} = 0.925$. The maximum deviation of the final result is then taken as an estimate of the systematic error. For the mean subjet multiplicities and for the ratio $r = \langle N_g - 1\rangle / \langle N_q - 1\rangle$, statistical errors are approximately twice as large as systematic errors over the entire range of y_0. For the n-subjet rates the systematic errors are comparable to or smaller than the statistical errors.

4. Results

Figure 2 shows the mean subjet multiplicity minus one for quark and gluon jets, $\langle N_q - 1\rangle$ and $\langle N_g - 1\rangle$. Error bars on the plots of final results are the quadratic sum of statistical and systematic uncertainties. Also shown on the figures are the predictions of the Monte Carlo models JETSET version 7.3 and HERWIG version 5.4 [11]. The ratio $r = \langle N_g - 1\rangle / \langle N_q - 1\rangle$ is shown in figure 3, along with the predictions of the above mentioned models as well as those of ARIADNE version 4.02 [12], and NLLjet version 2.0 [13]. (For a review of event generators see e.g. reference [14].) The important parameters of these models have been tuned using ALEPH data on charged particle inclusive and event-shape distributions [15] (see also [4]). Also shown are the predictions of a toy model based on JETSET, in which the colour charge for the parton splitting $g \to gg$ has been changed from 3 to 4/3, i.e. equal to that for the splitting $q \to qg$. The remaining parameters of the toy model were kept the same as used for the usual JETSET. This reproduces the main features of the data such as event-shape distributions and hadron multiplicities. For example, the mean charged multiplicity in the toy model is 20.4, compared to 20.8 in the standard JETSET model. A tuning of the toy model's parameters based on event-shape and inclusive charged-particle distributions resulted only in small changes in the predicted subjet rates and multiplicities, with e.g. an increase in the ratio r from 1.45 to 1.51 at $y_0 = 2 \cdot 10^{-3}$.

The measured quantities, are in generally good agreement with the QCD based models and in significant disagreement with the toy model. In particular, the measured multiplicity ratio $r = \langle N_g - 1\rangle / \langle N_q - 1\rangle$ is in good agreement with the QCD models over the entire range of y_0, but is significantly higher than that of the toy model for intermediate values of y_0. For $y_0 = 2 \cdot 10^{-3}$, the multiplicity ratio r is measured to be $1.96 \pm 0.13 \pm 0.07$, and for $y_0 = 1.6 \cdot 10^{-5}$ one obtains $1.29 \pm 0.02 \pm 0.01$. The enhanced value at intermediate y_0 provides significant evidence for the higher colour charge of the gluon.

Although gluon jets are observed to have more subjets than quark jets at intermediate y_0, this fact does not result in a correspondingly large number of subjets at low y_0, i.e. when individual hadrons are resolved. The sensitivity to the QCD colour factor decreases for small y_0 where both the QCD based and toy models predict multiplicity ratios in the range $1.2 - 1.3$. As one would expect, the ratio $\langle N_g - 1\rangle / \langle N_q - 1\rangle = 1.29$ found for small y_0 $(1.6 \cdot 10^{-5})$ is similar to the value obtained by using all charged particles. The mean charged particle multiplicities in the quark and gluon jets are found to be $\langle N_q^{ch}\rangle = 8.94 \pm 0.07 \pm 0.09$ and $\langle N_g^{ch}\rangle = 10.89 \pm 0.14 \pm 0.13$. The systematic error here includes a 1% normalization uncertainty based on previous studies of the charged multiplicity distribution [16] as well as the error estimated by varying the cut on P_{jet}. The charged particle multiplicities give the ratio $r_{ch} = \langle N_g^{ch} - 1\rangle / \langle N_q^{ch} - 1\rangle = 1.246 \pm 0.028 \pm 0.014$. This is in qualitative agreement with results of other analyses based on individual hadron multiplicities [17, 18].

Some additional Monte Carlo studies have been carried out to investigate the origin of the enhancement in the gluon's subjet multiplicity. Figure 4(a) shows the mean subjet multiplicities for quark and gluon jets at both hadron and parton levels as predicted by the JETSET model.

One sees that hadron and parton levels are in good agreement as long as the subjet resolution parameter y_0 is greater than about 10^{-3}. This corresponds to the subjets being separated by a relative transverse momentum $k_\perp$ of approximately $\sqrt{y_0} \cdot E_{cm} \approx 3$ GeV. For lower y_0, the relative $k_\perp$ between subjet pairs decreases, corresponding to an increase in the effective strong coupling $\alpha_s(k_\perp^2)$ and a breakdown of the perturbative description. Non-perturbative (hadronization) effects then become important, as can be seen by the divergence of the hadron and parton level predictions.

Figure 4(b) shows the multiplicity ratio $r = \langle N_g - 1 \rangle / \langle N_q - 1 \rangle$ for JETSET and the toy model. At parton level, JETSET gives a maximum ratio of 1.81, whereas the toy model has a maximum of 1.27. The fact that the QCD based JETSET does not predict the asymptotic value of 9/4 at parton level is a result of the finite centre-of-mass energy. The finite energy effects are enhanced by the fact that the average gluon jet energy of 28.0 GeV is somewhat smaller than that of quark jets, 31.6 GeV. Monte Carlo studies also indicate that this energy difference is responsible for the drop in r as y_0 approaches y_1.

The enhancement of the ratio r from the expected value of one to 1.27 for the parton level of the toy model is the result of finite quark masses. This has been investigated by generating events with light and heavy primary quarks ($d\overline{d}$ and $b\overline{b}$) separately. For the $d\overline{d}$ events, the parton level ratio is approximately one over the entire range of y_0. Collinear gluon radiation in b-quark jets, however, is highly suppressed because of the large b-quark mass. The combination of event flavours from Z decays leads to the ratio shown in figure 4(b).

As can be seen from figure 4(b), hadronization effects also play a noticeable role in the multiplicity ratio, even for intermediate values of y_0. For $y_0 > 10^{-3}$ the hadron level ratio is $5 - 10\%$ higher than the parton level. Although the measured value of 1.96 is close to the QCD prediction of 9/4, part of the gluon jet's enhancement in multiplicity is seen to be related to hadronization effects. A possible explanation of these effects in the context of a string model such as JETSET is that the gluon jet results from two strings (flux tubes) connected to both the leading quark and antiquark, whereas a quark jet results from a single piece of string connected to the gluon. A similar effect is expected in the HERWIG cluster model, where a three-jet event leads to two sets of clusters, one extending from the leading quark to the hard gluon, the other from the gluon to the leading antiquark, so that the gluon jet receives contributions from both sets.

The n-subjet rates give similar information on the internal jet structure. For the quark jets shown in figure 5(a), the toy and QCD based models all predict similar rates, and all are in reasonably good agreement with the data. The prediction of the toy model is, in fact, expected to be largely unchanged with respect to the QCD case since the gluon radiation from quarks depends only on C_F, which in both cases is 4/3.

For the n-subjet rates of gluon jets shown in figure 5(b), the toy model with the reduced gluon colour charge predicts lower rates for higher numbers of subjets than the QCD based models (JETSET and HERWIG), corresponding to a shift of the rate curves towards lower y_0. The data are in good agreement with JETSET and HERWIG, and in significant disagreement with the toy model. Monte Carlo studies of the n-subjet rates on hadron and parton levels indicate a behavior similar to that already seen with the subjet multiplicities. That is, the hadron and parton levels are in good agreement for $y_0 > 10^{-3}$, and diverge for smaller values of y_0. Figures 5(a) and 5(b) show substantial differences between quark and gluon jets, with e.g. gluon and quark 2-subjet rates measured to be $R_2^g = 0.496 \pm 0.017 \pm 0.016$ and $R_2^q = 0.270 \pm 0.009 \pm 0.008$ at $y_0 = 2 \cdot 10^{-3}$, giving a ratio $R_2^g / R_2^q = 1.83 \pm 0.12 \pm 0.11$.

5. Conclusions

A sample of 1750 gluon jets from three-jet events with a purity of 94.6% has be selected by requiring evidence of long-lived heavy flavour hadrons in the two remaining jets. By considering all jets without tagging a second jet sample of 2/3 quark and 1/3 gluon jets is obtained. These samples are used to determine the subjet structure of pure quark and gluon jets. In particular, the subjet multiplicities and rates for quark and gluon jets have been measured and compared to theoretical predictions, showing a significant indication for the higher colour charge of the gluon. Clear differences are observed between quark and gluon jets. The subjet multiplicity ratio of gluon to quark jets $\langle N_g - 1\rangle/\langle N_q - 1\rangle$, predicted to be $C_A/C_F = 9/4$ in leading order QCD, is measured to be 1.96 ± 0.15 for $y_0 = 2 \cdot 10^{-3}$, but falls to 1.29 ± 0.03 for $y_0 = 1.6 \cdot 10^{-5}$, where the errors are the quadratic sums of statistical and systematic uncertainties. This value as well as other aspects of the internal structure of quark and gluon jets can be understood to result from both perturbative and non-perturbative effects. A high sensitivity to the parton colour charge is only found when the subjets are resolved with a sufficiently large resolution parameter ($y_0 > 10^{-3}$) such that non-perturbative effects remain small.

Acknowledgements

We are very grateful to B.R. Webber and T. Sjöstrand for useful discussions. We wish to thank our colleagues from the accelerator divisions for the successful operation of LEP. We are indebted to the engineers and technicians in all our institutions for their contribution to the good performance of ALEPH. Those of us from non-member countries thank CERN for its hospitality.

References

[1] W.J. Stirling, J. Phys. **G** Nucl. Part. Phys. **17** (1991) 1567.

[2] G. Altarelli, Phys. Rep. **81** (1982) 1.

[3] S. Catani, B.R. Webber, Yu.L. Dokshitzer, and F. Fiorani, Nucl. Phys. **B383** (1992) 419; Nucl. Phys. **B377** (1992) 445.

[4] The ALEPH Collaboration, *Study of Sub-jet Multiplicities in Hadronic Z Decays*, contribution to the 26th International Conference on High Energy Physics, Dallas, Texas, 1992.

[5] O. Adriani et al., (L3) Phys. Rep. **236** (1993) 207.

[6] R. Akers et al., (OPAL) *A study of mean sub-jet multiplicities in two- and three-jet hadronic Z^0 decays*, CERN-PPE/94-52, 1994.

[7] D. Decamp et al., (ALEPH) Nucl. Instr. Meth. A **294** (1990) 121.

[8] D. Decamp et al., (ALEPH) Phys. Rep. **216** (1992) 253;
D. Buskulic et al., (ALEPH) *Performance of the* ALEPH *Detector at LEP*, CERN-PPE/94-170, 1994.

[9] D. Decamp et al., (ALEPH) Phys. Lett. **B 313** (1993) 535.

[10] M. Bengtsson and T. Sjöstrand, Phys. Lett. **B 185** (1987) 435.

[11] G. Marchesini, B.R. Webber, G. Abbiendi, I.G. Knowles, M.H. Seymour and J. Chyla, Computer Physics Communications **67** (1992) 465.

[12] L. Lönnblad, Computer Physics Communications **71** (1992) 15.

[13] K. Kato and T. Munehisa, Computer Physics Communications **64** (1991) 67, Mod. Phys. Lett. **A 1** (1986) 345, Phys. Rev. **D 36** (1987) 61, Phys. Rev. **D 39** (1989) 156.

[14] Z Physics at LEP I, Volume 3: Event Generators and Software, G. Altarelli, R. Kleiss and C. Verzegnassi, ed., CERN 89-08 (1989) 143.

[15] D. Buskulic et al., (ALEPH) Z. Phys. **C 55** (1992) 209.

[16] D. Decamp et al., (ALEPH) Phys. Lett. B273 (1991) 181.

[17] G. Alexander et al., (OPAL) Phys. Lett. **B 265** (1991) 462;
P.D. Acton et al., (OPAL) Z. Phys. **C 58** (1993) 387.

[18] The ALEPH Collaboration, *Quark-Gluon Jet Properties with a Lifetime Tag in ALEPH*, contribution to the 27*th* International Conference on High Energy Physics, Glasgow, Scotland (1994) reference number GLS0539.

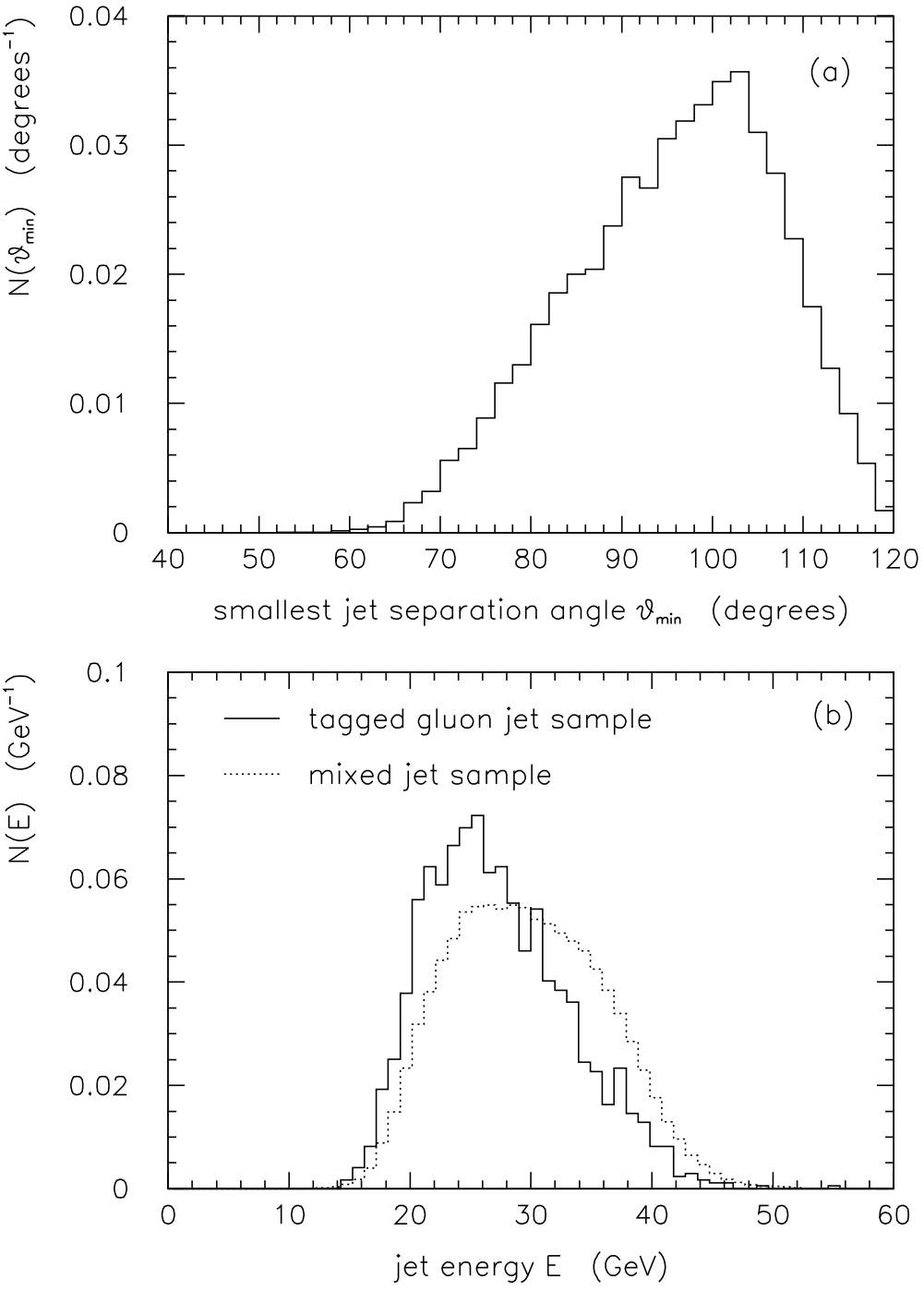

Figure 1: (a) Distribution of the smallest separation angle between jets θ_{min} in all three-jet events. (b) Distribution of jet energies in the tagged and mixed gluon samples. All distributions are normalized to unit area.

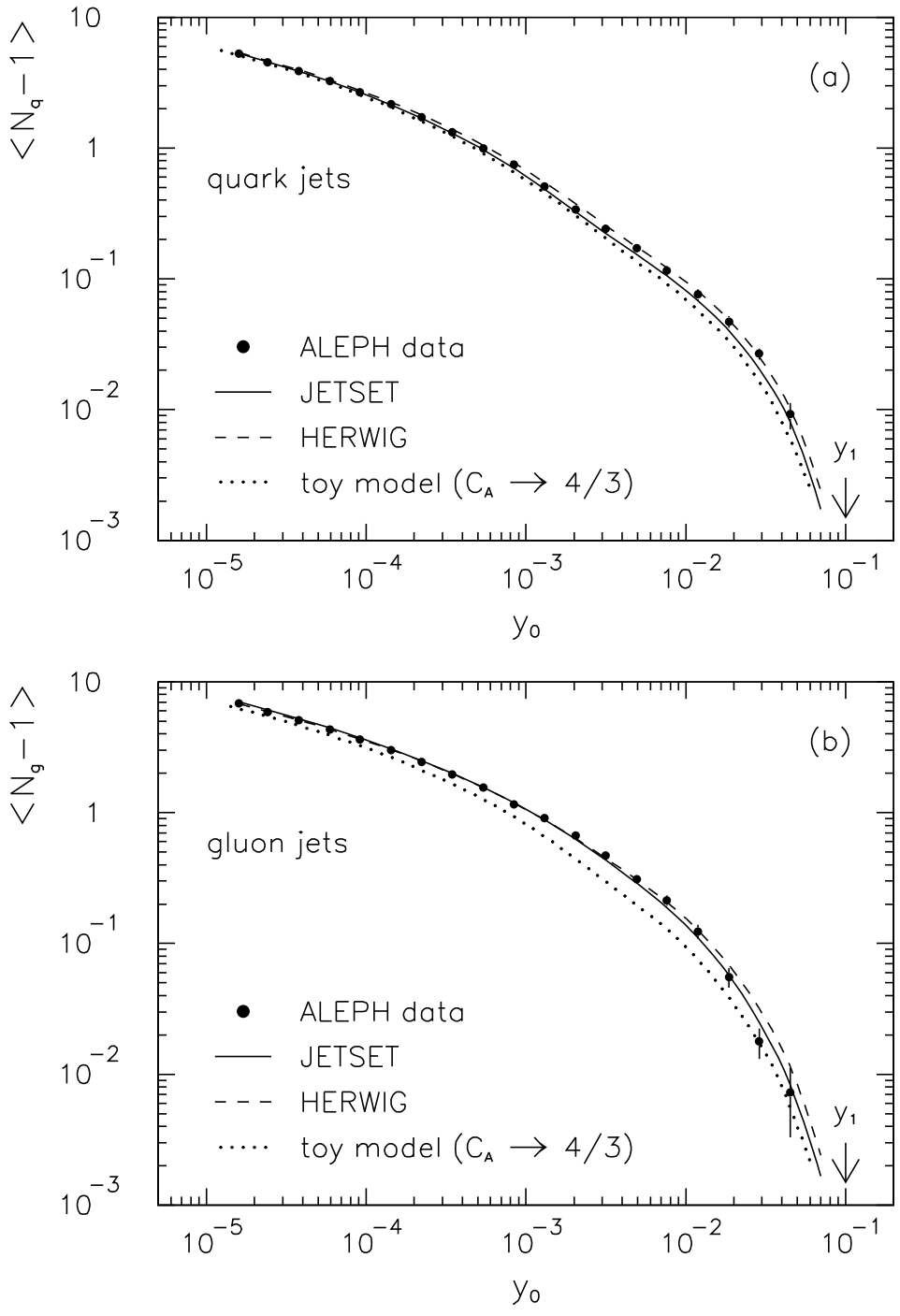

Figure 2: Measured mean subjet multiplicity minus one (points) for (a) quark jets $\langle N_q - 1 \rangle$ and (b) gluon jets $\langle N_g - 1 \rangle$ as a function of the subjet resolution parameter y_0. Also shown are the predictions of various Monte Carlo models (curves).

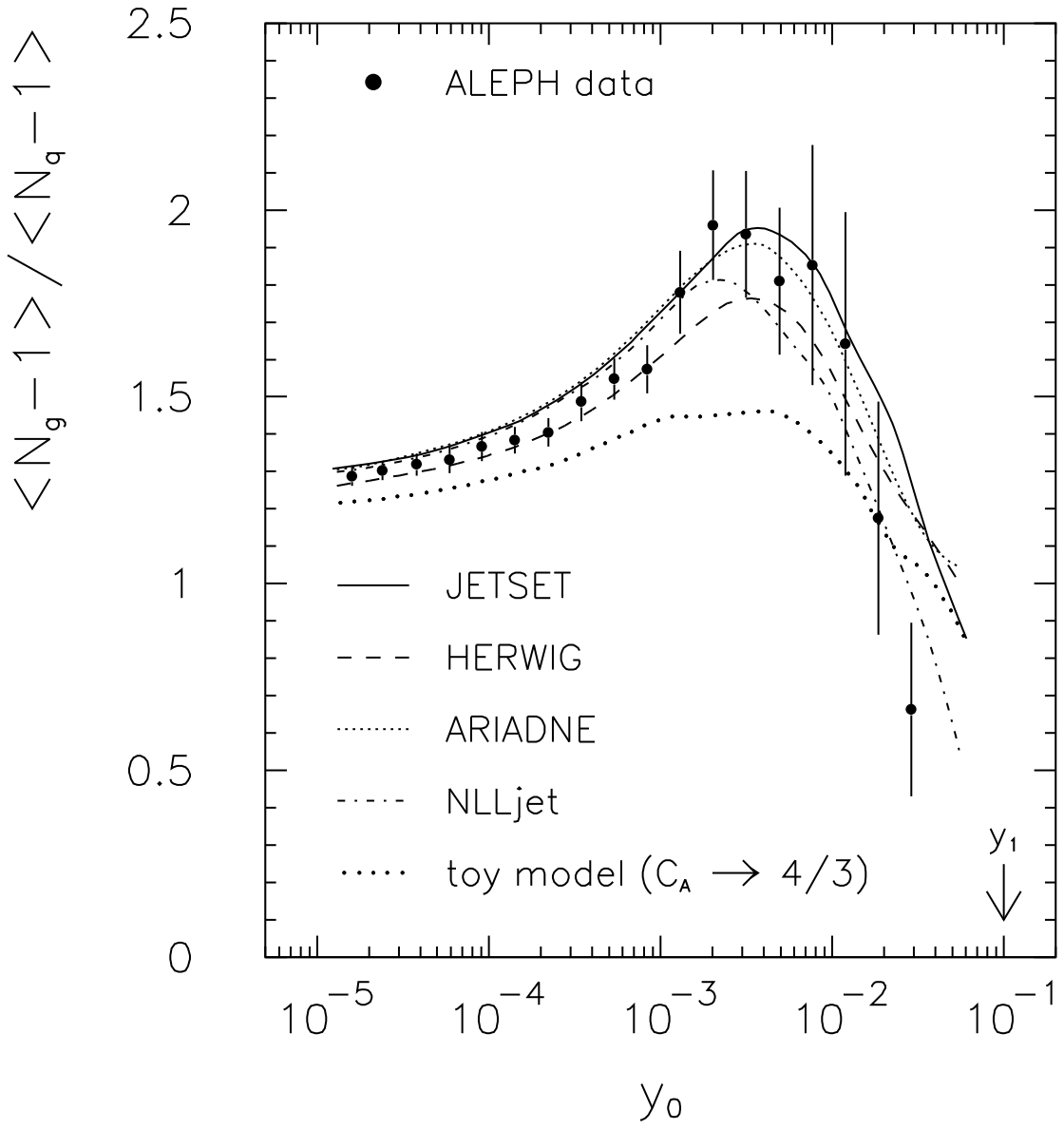

Figure 3: Measured ratios of subjet multiplicities minus one $\langle N_g - 1 \rangle / \langle N_q - 1 \rangle$ for gluon and quark jets (points) with the predictions of various Monte Carlo models (curves) as a function of the subjet resolution parameter y_0.

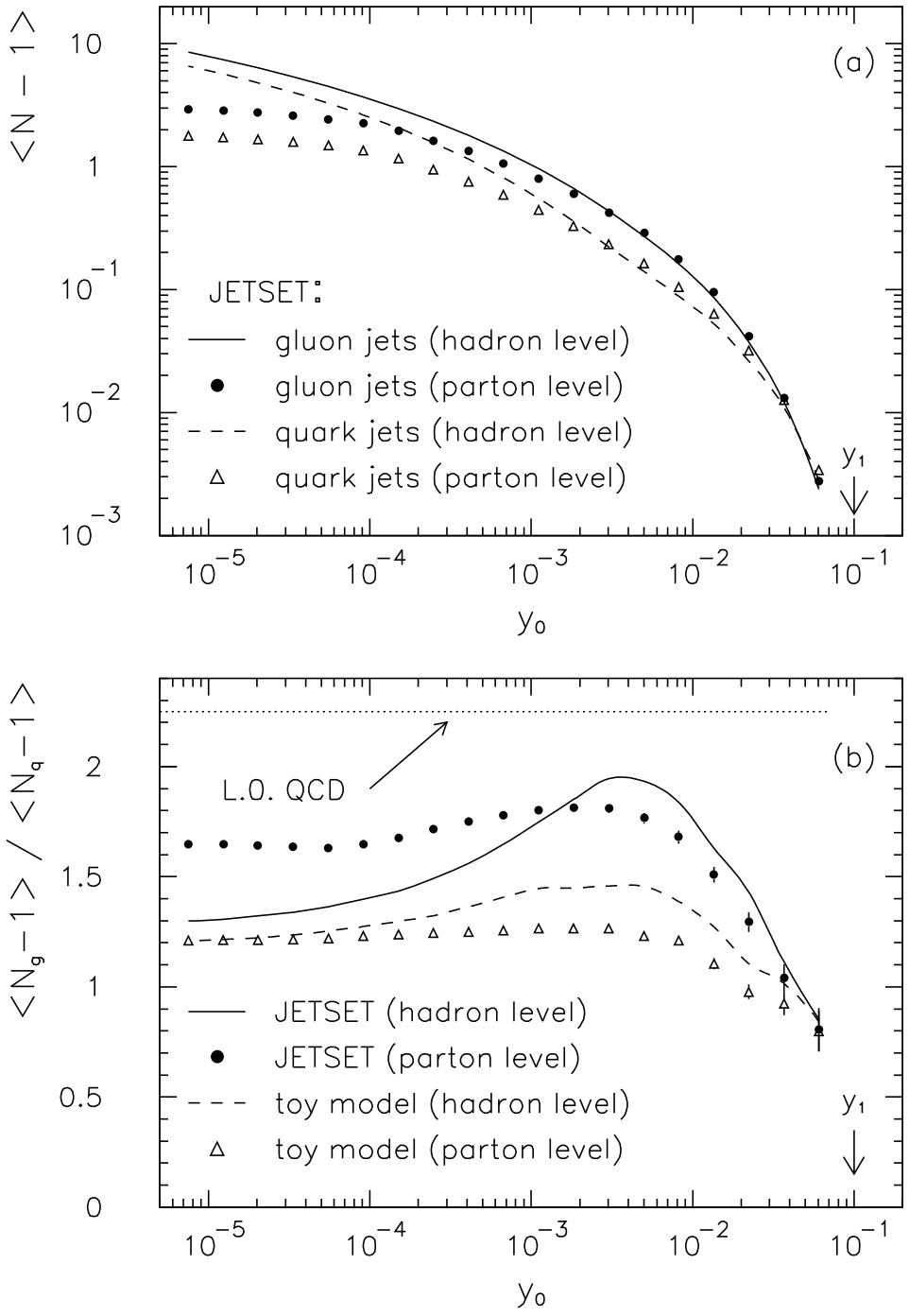

Figure 4: (a) Mean subjet multiplicities for quark and gluon jets on both hadron and parton levels as predicted by the JETSET model. (b) The ratio of mean subjet multiplicities $\langle N_g - 1\rangle / \langle N_q - 1\rangle$ obtained from JETSET and from a toy model in which the gluon's color charge C_A was reduced from 3 to 4/3. Also shown is the prediction of leading order QCD, $C_A/C_F = 9/4$.

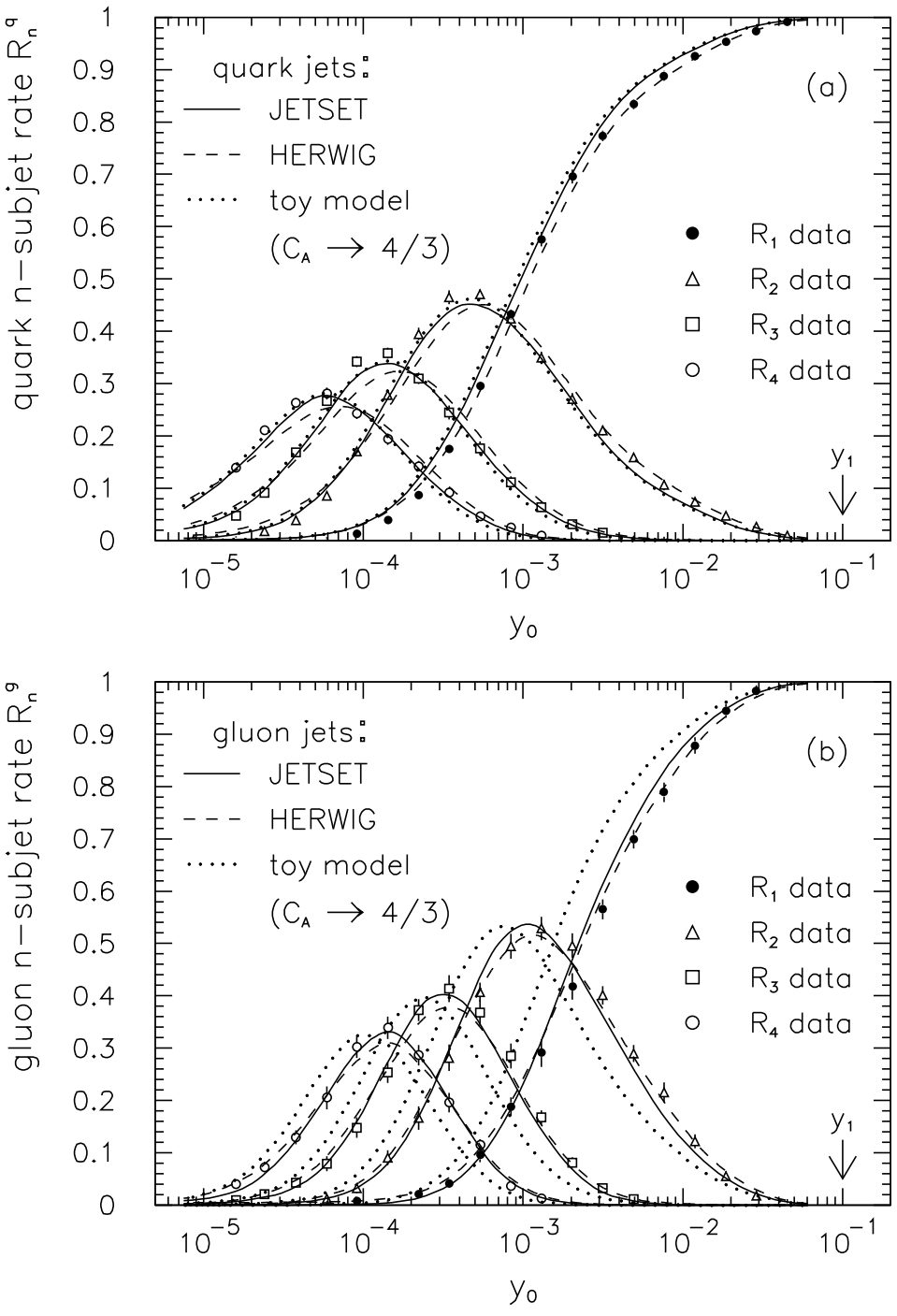

Figure 5: Measured n-subjet rates R_n for (a) quark jets and (b) gluon jets (points) as a function of the subjet resolution parameter y_0. Also shown are the predictions of various Monte Carlo models (curves).